Rock Mech. Rock Engng. (2006) 39 (4), 339–358
DOI 10.1007/s00603-005-0068-1

Rock Mechanics and Rock Engineering
Printed in Austria

Statistics of Boulder Encounters during Shaft Excavation

By

D. Veneziano[1] and **J. Van Dyck**[2]

[1] Department of Civil and Environmental Engineering, MIT, Cambridge, MA, U.S.A.
[2] Department of Civil Engineering, KULeuven, Louvain, Belgium

Received December 12, 2004; accepted June 21, 2005
Published online August 19, 2005

Summary

We study the problem of boulder encounter during shaft excavation and the bias that results from directly using statistics from borehole samples without correction for probe diameter. We specifically focus on two quantities, the rate of boulder encounters λ_1 and the total length of obstructed shaft drilling L_1. Assuming that boulders have spherical shape or cylindrical shape of a particular type, we evaluate how λ_1 and the mean and variance of L_1 depend on the shaft diameter, the distribution of the boulder diameter, and the minimum boulder diameter that constitutes an obstruction to drilling. The statistics on L_1 assume that the boulder centers are distributed according to a homogeneous Poisson process in space. Finally, we briefly discuss the problem of inferring the spatial density of boulders and their diameter distribution from borehole data. Both λ_1 and L_1 increase significantly with increasing shaft diameter; hence the uncorrected statistics from borehole samples severely under-predict these two quantities during large-shaft drilling. Moreover, for typical parameter values, the mean value of L_1 may be a significant fraction of the total shaft length.

Keywords: Shaft excavation, boulders, borehole data, statistical modeling, Poisson process, sampling exploration.

1. Introduction

It is often observed that the rate of boulder encounter during shaft excavation is greater than that determined from initial borings. This is a frequent cause of litigation, cost overruns and construction delays.

It would be desirable to have a quantitative understanding of the problem including statistical variability, quantify the bias when directly using borehole results as representative of shaft drilling conditions, and determine when a claim of excessive shaft excavation obstruction is legitimate.

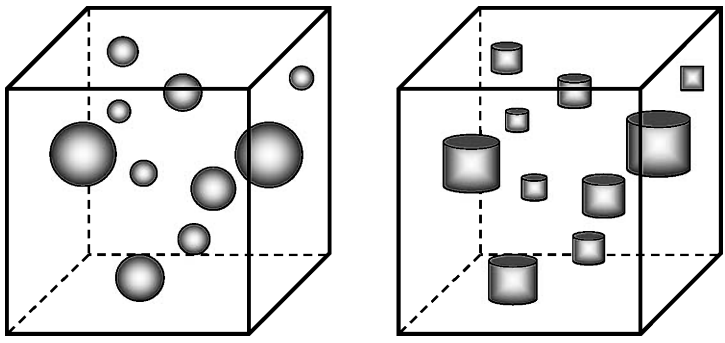

(a) spherical boulders *(b) cylindrical boulders*

Fig. 1. Illustration of spherical and cylindrical boulder models

We address these issues for the case when obstructions are caused by spherical boulders with random diameter and homogeneous Poisson distribution in space, as illustrated in Fig. 1a. ''Homogeneous Poisson distribution'' means that the centers of the boulders are equally likely to be anywhere in the geologic medium and different boulders have independent locations. This simplifying assumption neglects the fact that in reality the boulders do not overlap. Results are derived also under the condition that the boulders have a cylindrical shape with vertical axis (parallel to the shaft) and random height equal to the base diameter (see Fig. 1b), and for some variants of the above spherical and cylindrical cases. Another assumption we make is that no boulder protrudes above the soil surface. Although idealized, these models can be used to generate approximations to physical situations when the boulders have more complicated shapes, dependent locations, and non-homogeneous spatial distribution.

The analytical results depend on known drilling parameters such as the length and diameter of the shaft and the minimum size of boulders that constitute obstructions, as well as unknown parameters of the boulder field (the mean spatial density λ and the diameter distribution F_D). Hence another important problem is how to use boring information to estimate λ and F_D.

Section 2 presents analytical results for the process of boulder encounters as drilling of the shaft progresses. Results in this section apply to both spherical and cylindrical boulders. Section 3 deals with the problem of estimating the length of obstructed drilling, L_1, whose distribution depends on the shape of the boulders. We obtain the mean value and variance of L_1 for both spherical and cylindrical boulders and show how the shaft diameter affects these statistics. Section 4 considers the inference of λ and F_D from borehole data and Section 5 summarizes the main findings of the study and suggests extensions.

2. Rate of Boulder Encounters

Throughout the paper we assume that, when projected on a horizontal plane, boulders appear as circular discs of radius D. For the results derived in this section, no other geometrical characteristic of the boulders matters. In particular, the results apply to

both spherical and cylindrical boulders. Other quantities used in the present analysis are:

$d_{\min}$ = minimum diameter of boulders that constitute obstructions;
λ = mean spatial density of boulders with $D \geq d_{\min}$ (the expected number of obstructing-boulder centers per unit volume);
$f_D(x) = \frac{dF_D(x)}{dx}$ = probability density function of $[D|D \geq d_{\min}]$ for the obstructing boulders; and
m_D, σ_D^2, $V_D = \sigma_D/m_D$ = mean value, variance, and coefficient of variation of $[D|D \geq d_{\min}]$, respectively.

Hereafter, we shall refer to obstructing boulders simply as "boulders" and use D for the conditional random variable $[D|D \geq d_{\min}]$. When the distinction between the distributions of D for $d_{\min} = 0$ and $d_{\min} > 0$ is needed, we shall refer to these as the "untruncated" and "truncated" boulder diameter distribution, respectively.

We are interested in the boulder encounter rate when drilling a shaft or borehole of diameter d_s. One may define two such encounter rates: the "linear rate" $\lambda_1(d_s)$ = expected number of boulder encounters per unit length advancement when drilling a shaft or borehole of diameter d_s, and the "volumetric rate" $\lambda_3(d_s)$ = expected number of boulder encounters per unit excavated volume when drilling a shaft or borehole of diameter d_s.

The linear rate is obtained by observing that the mean number of boulders encountered per unit length of shaft equals the mean number of boulder centers in a cylinder of unit height, circular base, and base diameter $(D + d_s)$. Hence

$$\lambda_1(\mathrm{d_s}) = \frac{\pi}{4}\lambda \int_{\mathrm{d_{min}}}^{\infty} (\mathrm{x} + \mathrm{d_s})^2 \mathrm{f_D(x)dx} = \frac{\pi}{4}\lambda[\sigma_{\mathrm{D}}^2 + (\mathrm{m_D} + \mathrm{d_s})^2] \tag{1}$$

The volumetric rate is obtained by dividing the linear rate by the area of the circular shaft,

$$\lambda_3(d_s) = \frac{4}{\pi d_s^2}\lambda_1(d_s) = \frac{1}{d_s^2}\lambda[\sigma_D^2 + (m_D + d_s)^2] \tag{2}$$

To better understand Eqs. (1) and (2), consider the case when all the boulders have the same diameter D. For this special case Eqs. (1) and (2) reduce to

$$\lambda_1(d_s) = \frac{\pi}{4}\lambda(D + d_s)^2 \tag{3}$$

$$\lambda_3(d_s) = \frac{1}{d_s^2}\lambda(D + d_s)^2 \tag{4}$$

It is convenient to introduce two dimensionless quantities, $\gamma_{\lambda_1}(d_s/D)$ and $\gamma_{\lambda_3}(d_s/D)$, as the following encounter-rate ratios:

$$\gamma_{\lambda_1}(d_s/D) = \frac{\lambda_1(d_s, D)}{\lambda_1(d_s = 0, D)} = \left(1 + \frac{d_s}{D}\right)^2 \tag{5}$$

$$\gamma_{\lambda_3}(d_s/D) = \frac{\lambda_3(d_s, D)}{\lambda_3(d_s = \infty, D)} = \frac{\lambda_3(d_s, D)}{\lambda} = \left(1 + \frac{D}{d_s}\right)^2 \tag{6}$$

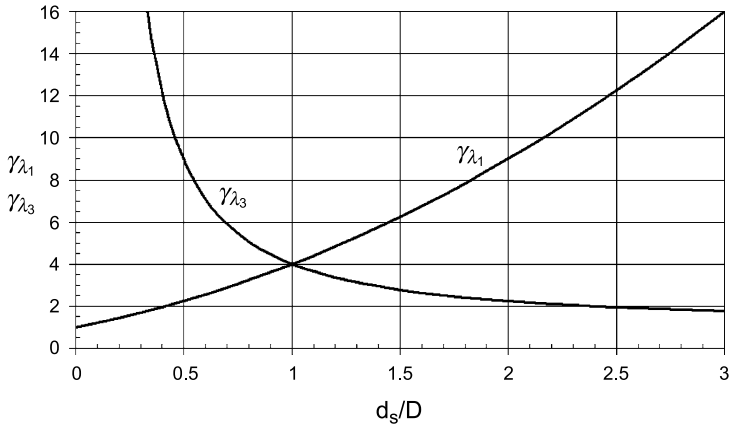

Fig. 2. Factors γ_{λ_1} and γ_{λ_3} in Eqs. (5) and (6) for boulders of identical diameter D and shaft diameter d_s

Hence $\gamma_{\lambda_1}(d_s/D)$ is the factor by which the linear encounter rate of boulders of diameter D is increased when drilling a shaft of diameter d_s compared to drilling a borehole of zero (or very small) diameter. Similarly, $\gamma_{\lambda_3}(d_s/D)$ is the factor by which the volumetric rate of boulders of diameter D is increased when drilling a shaft of diameter d_s as opposed to a shaft of infinite diameter. The latter volumetric rate equals λ, the mean spatial density of obstructing boulder centers.

The factors $\gamma_{\lambda_1}(d_s/D)$ and $\gamma_{\lambda_3}(d_s/D)$ have opposite dependence on the diameter ratio d_s/D. For example, for shaft diameters $d_s = D$ and $d_s = 2D$, Eq. (5) shows that the linear rate of encounters is respectively 4 and 9 times the rate for a borehole of very small diameter. For the same diameters, Eq. (6) shows that the volumetric encounter rate is larger than λ by a factor of respectively 4 and $(1.5)^2 = 2.25$. Plots of $\gamma_{\lambda_1}(d_s/D)$ and $\gamma_{\lambda_3}(d_s/D)$ for d_s/D in the range [0, 3] are shown in Fig. 2.

Factors analogous to $\gamma_{\lambda_1}(d_s/D)$ and $\gamma_{\lambda_3}(d_s/D)$ can be obtained also for the general case when the boulder diameter D is random. In this case γ_{λ_1} and γ_{λ_3} depend on two parameters, the ratio d_s/m_D between the shaft diameter and the mean boulder diameter and the coefficient of variation of the boulder diameter, $V_D = \sigma_D/m_D$:

$$\gamma_{\lambda_1}\left(\frac{d_s}{m_D}, V_D\right) = \frac{\lambda_1(d_s)}{\lambda_1(d_s=0)} = \frac{\sigma_D^2 + (m_D + d_s)^2}{\sigma_D^2 + m_D^2} = \frac{(1+\frac{d_s}{m_D})^2 + V_D^2}{1 + V_D^2} \tag{7}$$

$$\gamma_{\lambda_3}\left(\frac{d_s}{m_D}, V_D\right) = \frac{\lambda_3(d_s)}{\lambda_3(d_s=\infty)} = \left(1 + \frac{m_D}{d_s}\right)^2 + V_D^2\left(\frac{m_D}{d_s}\right)^2 \tag{8}$$

For $V_D = 0$, Eqs. (7) and (8) reduce to Eqs. (5) and (6). The factors $\gamma_{\lambda_1}\left(\frac{d_s}{m_D}, V_D\right)$ and $\gamma_{\lambda_3}\left(\frac{d_s}{m_D}, V_D\right)$ are plotted in Fig. 3 using a format similar to Fig. 2. The curves in each panel of Fig. 3 are for different values of the coefficient of variation V_D. For λ, m_D and d_s fixed, the linear rate of encounters λ_1 increases with increasing σ_D^2 (hence with increasing V_D); see Eq. (1). However, as one can see from Fig. 3a, as V_D increases the sensitivity of λ_1 to d_s/m_D decreases. Hence the correction from borehole

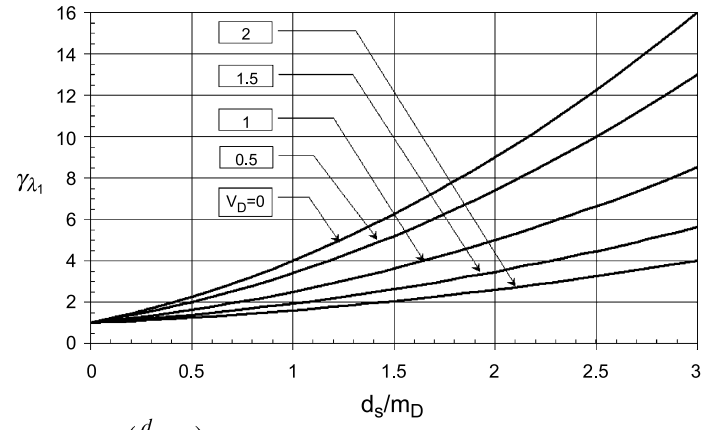

(a) Factor $\gamma_{\lambda_1}\left(\frac{d_s}{m_D}, V_D\right)$

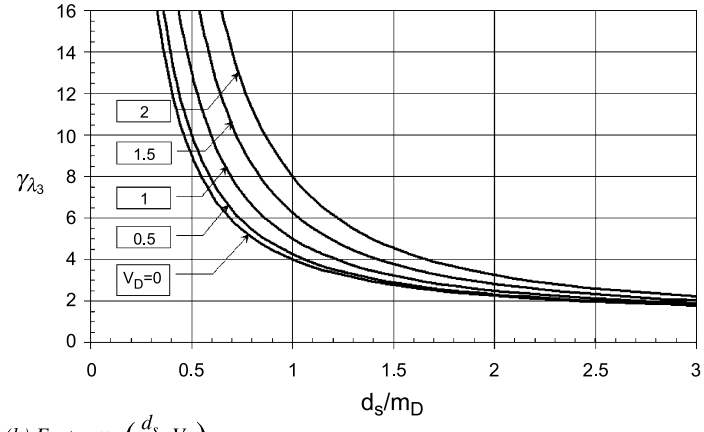

(b) Factor $\gamma_{\lambda_3}\left(\frac{d_s}{m_D}, V_D\right)$

Fig. 3. Factors γ_{λ_1} and γ_{λ_3} in Eqs. (7) and (8) for boulders with random diameter D. m_D and V_D are the mean value and coefficient of variation of the conditional boulder diameter $[D|D \geq d_{\min}]$ and d_s is the shaft diameter

to shaft drilling is not as large as in the case when the diameter is deterministic. For example, for $d_s = 2m_D$, the factor γ_{λ_1} equals 9 for $V_D = 0$ but only 5 for $V_D = 1$. In the case of boulders with exponentially distributed diameter and obstruction cutoff $d_{\min}$, the coefficient of variation of D is $V_D = \frac{m_{D_U}}{d_{\min} + m_{D_U}} = 1 - \frac{d_{\min}}{m_D}$, where m_{D_U} and $m_D = m_{D_U} + d_{\min}$ are the ''untruncated'' mean value of $(D|D > 0)$ and the ''truncated'' mean value of $(D|D > d_{\min})$, respectively. (For other relations between the untruncated and truncated moments of the exponential distribution, see Appendix A.) For example, $V_D = 0.5$ if $d_{min} = m_{D_U}$, whereas $V_D = 1$ in the untruncated case $d_{\min} = 0$. The factor γ_{λ_3} shows an opposite dependence on V_D; see Fig. 3b.

The rate $\lambda_1(d_s)$ in Eq. (1) and all other results in this section do not depend on whether the boulder locations are Poisson or not. Under the Poisson assumption,

$\lambda_1(d_s)$ determines completely the probability distribution of the number $N_{new}(L)$ of new boulder encounters when drilling a shaft of length L. The qualifier "new" is needed here because we exclude boulders that might appear at the ground surface when excavation begins, i.e. boulders that might cause obstruction at depth $z = 0$. The distribution of $N_{new}(L)$ is Poisson, with mean value

$$E[N_{new}(L)] = \lambda_1(d_s)L = \frac{\pi}{4}\lambda[\sigma_D^2 + (m_D + d_s)^2]L \tag{9}$$

With this information, it is for example easy to obtain the probability that the number of new boulder encounters $N_{new}(L)$ exceeds any given value.

3. Length of Obstructed Drilling

Now we turn to studying the length of obstructed shaft drilling, which is a quantity of great interest in practice. As before, a shaft or borehole of diameter d_s is drilled to a depth L in a geologic medium with embedded boulders. The centers of the boulders are generated by a homogeneous Poisson point process in space with intensity λ and boulder diameters $D \geq d_{\min}$ have a probability distribution F_D with density f_D.

When a boulder i of diameter $D_i \geq d_{\min}$ is encountered, drilling slows down over the "obstructed segment" S_{1_i} obtained by intersecting the boulder with the shaft and projecting the intersection on the shaft axis; see Fig. 4a for a two-dimensional illustration. Only boulders with diameter larger than $d_{\min}$ are assumed to cause drilling delays. The subset of the shaft axis where excavation is obstructed, S_1, is the union of the segments S_{1_i}, i.e. $S_1 = \cup_i S_{1_i}$; see Fig. 4b. Hence the total length of obstructed excavation, $L_1 = length(S_1)$, ranges from 0 to L.

We are interested in the mean value and variance of L_1 given the length of the shaft L and its diameter d_s, the mean spatial density of boulders λ and the probability

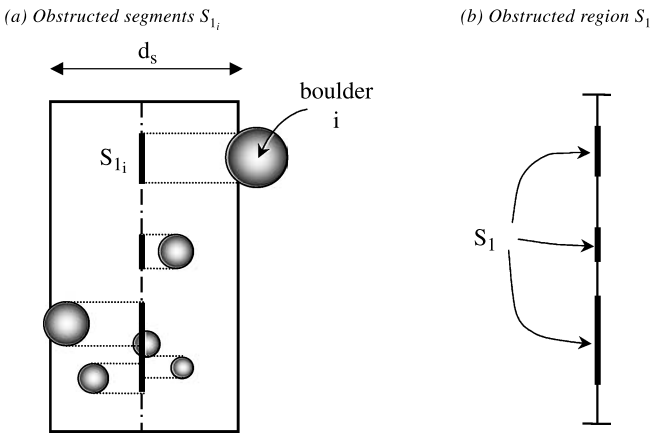

Fig. 4. Schematic 2D illustration of the obstructed excavation sets S_{1_i} and S_1

density of their diameter f_D, and the minimum diameter that causes obstruction $d_{\min}$. Recall that f_D is the probability density of the conditional random variable $[D|D \geq d_{\min}]$. This problem does not seem to have been previously studied, although it bears some resemblance to other problems of projections of interceptions of solids with random distributions of spheres. For example, significant work has been done on thin sections of media with embedded random spheres; see Stoyan et al. (1995), Sec. 11.4.3, for a review.

In the analysis that follows we use the following notation:

$$\begin{aligned} \mathrm{I(z)} &= \text{indicator variable with value 1 if drilling at depth z is obstructed (if } z \in S_1\text{)} \\ &\quad \text{and value 0 if drilling at depth z is unobstructed} \\ P_0 &= P[I(z) = 0] \text{ (notice: } P_0 \text{ is not a function of z)} \\ P_1 &= P[I(z) = 1] = 1 - P_0 \\ P_{ij}(\Delta) &= P[(I(z) = i) \cap (I(z + \Delta) = j)], \text{ i, j} = 0,1 \end{aligned}$$

where Δ is some increment of z. Hence P_0 and P_1 are the probabilities of unobstructed and obstructed excavation at the generic depth z and for example $P_{00}(\Delta)$ is the probability that excavation is unobstructed at both depths z and $\mathrm{z} + \Delta$.

We start by studying the case of spherical boulders and then consider boulders with cylindrical and other shapes.

3.1 Spherical Boulders

In analyzing the problem for spherical boulders we need the volume of certain solids of revolution. One is the solid obtained by revolving the shaded planar figure in Fig. 5a around the z axis. We denote this solid by Ω(D) and its volume by V(D). (As the figure indicates, Ω and V depend also on the shaft diameter d_s, but in our analysis d_s is controlled and kept fixed.)

The other solid, $\Omega_\Delta(D)$, is the union of two copies of Ω(D) translated by Δ relative to each other along the z axis. Hence $\Omega_\Delta(D)$ is the solid obtained by revolving the

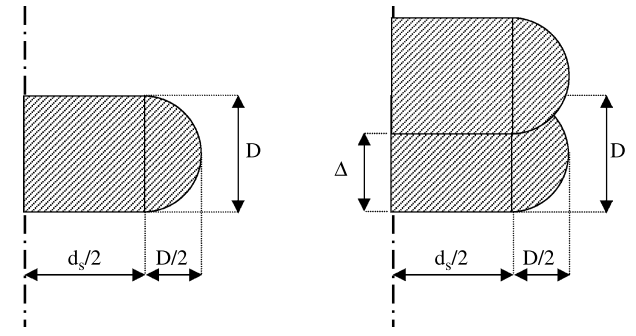

(a) Generator of solid $\Omega(D)$ *(b) Generator of solid* $\Omega_\Delta(D)$

Fig. 5. The solids $\Omega(D)$ and $\Omega_\Delta(D)$ are obtained by revolving the shaded planar figures in (**a**) and (**b**) around the z axis

shaded planar figure in Fig. 5b around the z axis. The volume of $\Omega_\Delta(D)$ is denoted by $V_\Delta(D)$. It is shown in Appendix B that

$$V(D) = \frac{\pi}{4}\left(d_s^2 D + \frac{\pi}{2} d_s D^2 + \frac{2}{3} D^3\right)$$

$$V_\Delta(D) = \begin{cases} 2V(D), & \text{if } \Delta \geq D \\ \dfrac{\pi}{4}\left\{(d_s^2 + D^2)(D+\Delta) - \dfrac{1}{3}(D^3 + \Delta^3)\right\} & \\ + \dfrac{\pi}{4} d_s D^2 \left\{\pi - \arccos\left(\dfrac{\Delta}{D}\right) + \dfrac{\Delta}{D}\sqrt{1 + \left(\dfrac{\Delta}{D}\right)^2}\right\}, & \text{if } \Delta < D \end{cases} \tag{10}$$

Now we turn to the mean value and variance of L_1.

(a) Mean Value of L_1

The length L_1 may be written as the integral

$$L_1 = \int_0^L I(z)dz \tag{11}$$

where I(z) is the indicator variable of obstructed drilling at depth z; see notation above. It follows from Eq. (11) that the mean value of L_1 is

$$E[L_1] = E[I(z)]L = P_1 L = (1 - P_0)L \tag{12}$$

The probability of no obstruction at depth z, P_0, is the probability that, for all $D \geq d_{\min}$, no boulder has its center inside a region $\Omega(D)$ whose volume V(D) is given in Eq. (10). Using standard properties of the Poisson process,

$$P_0 = exp\{-\lambda E[V(D)]\} = exp\left\{-\frac{\pi}{4}\lambda\left(d_s^2 E[D] + \frac{\pi}{2} d_s E[D^2] + \frac{2}{3} E[D^3]\right)\right\} \tag{13}$$

Substitution of Eq. (13) into Eq. (12) finally gives

$$E[L_1] = L\left\{1 - exp\left[-\overline{N}_{d_s}\left(\frac{E[D]}{d_s} + \frac{\pi}{2}\frac{E[D^2]}{d_s^2} + \frac{2}{3}\frac{E[D^3]}{d_s^3}\right)\right]\right\} \tag{14}$$

where $\overline{N}_{d_s} = \frac{\pi}{4}\lambda d_s^3$ is the expected number of boulder centers inside a cylinder of height d_s, circular basis, and basis diameter d_s.

It is interesting to compare this mean obstructed length for a shaft of diameter d_s with the same quantity for a borehole of very small (mathematically, zero) diameter. The ratio γ_{L_1} between the two expected lengths is the bias factor if one uses the unmodified borehole results to predict the obstructed length during shaft drilling. This bias factor is

$$\gamma_{L_1} = \frac{E[L_1(d_s)]}{E[L_1(d_s = 0)]} = \frac{1 - exp\left[-\overline{N}_{d_s}\left(\dfrac{E[D]}{d_s} + \dfrac{\pi}{2}\dfrac{E[D^2]}{d_s^2} + \dfrac{2}{3}\dfrac{E[D^3]}{d_s^3}\right)\right]}{1 - exp\left[-\dfrac{2}{3}\overline{N}_{d_s}\dfrac{E[D^3]}{d_s^3}\right]} \tag{15}$$

To make Eqs. (14) and (15) more transparent, we consider first the simpler case when all boulders have the same diameter D. Then $E[D^r] = D^r$ and Eqs. (14) and (15) reduce to

$$E[L_1] = L\left(1 - \exp\left\{-\overline{N}_{d_s}\left[\frac{D}{d_s} + \frac{\pi}{2}\left(\frac{D}{d_s}\right)^2 + \frac{2}{3}\left(\frac{D}{d_s}\right)^3\right]\right\}\right)$$

$$\gamma_{L_1}\left(\frac{d_s}{D}, \overline{N}_{d_s}\right) = \frac{1 - \exp\left\{-\overline{N}_{d_s}\left[\frac{D}{d_s} + \frac{\pi}{2}\left(\frac{D}{d_s}\right)^2 + \frac{2}{3}\left(\frac{D}{d_s}\right)^3\right]\right\}}{1 - \exp\left[-\frac{2}{3}\overline{N}_{d_s}\left(\frac{D}{d_s}\right)^3\right]} \tag{16}$$

where $\overline{N}_{d_s} = \frac{\pi}{4}\lambda d_s^3$, as in Eq. (14). Figures 6a and b show plots of the expected obstructed fraction $E[L_1]/L$ and bias factor $\gamma_{L_1}(\frac{d_s}{D}, \overline{N}_{d_s})$ in Eq. (16) as a

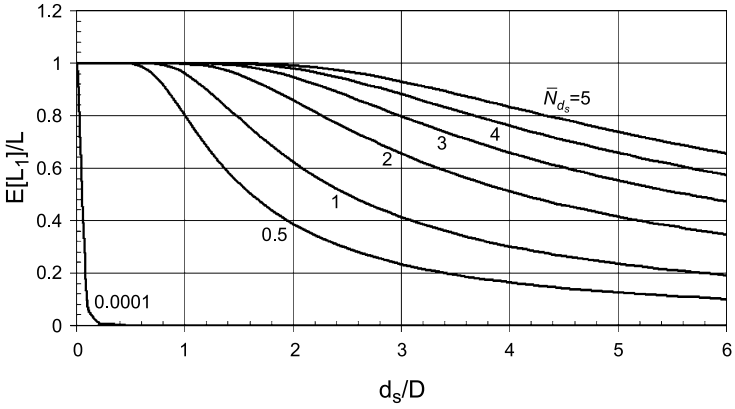

(a) Expected obstructed fraction $E[L_1]/L$

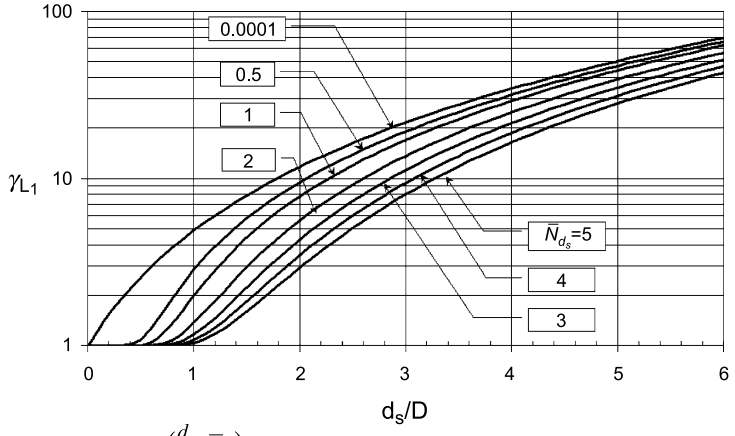

(b) Bias factor $\gamma_{L_1}\left(\frac{d_s}{D}, \overline{N}_{d_s}\right)$

Fig. 6. Expected obstructed fraction $E[L_1]/L$ and bias factor $\gamma_{L_1}(\frac{d_s}{D}, \overline{N}_{d_s})$ in Eq. (16) as a function of the normalized shaft diameter d_s/D for different values of the expected number $\overline{N}_{d_s} = \frac{\pi}{4}\lambda d_s^3$ in Eq. (14). Case of spherical boulders with identical diameter D

function of the normalized shaft diameter d_s/D for different values of the expected number $\overline{N}_{d_s}$.

For high values of $\overline{N}_{d_s}$ and small d_s/D ratios (meaning large and densely distributed boulders), the expected obstructed fraction $E[L_1]/L$ saturates to 1. Also for $\overline{N}_{d_s}$ as low as 2 and d_s/D as high as 4, Fig. 6a shows that about one half of the shaft excavation length is expected to be obstructed.

Consider now the bias factor $\gamma_{L_1}(\frac{d_s}{D}, \overline{N}_{d_s})$ in Fig. 6b. For $\overline{N}_{d_s}$ close to 0, Taylor expansion of Eq. (16) gives

$$\gamma_{L_1}\left(\frac{d_s}{D}, \overline{N}_{d_s} \approx 0\right) \approx 1 + \frac{3\pi}{4}\left(\frac{d_s}{D}\right) + \frac{3}{2}\left(\frac{d_s}{D}\right)^2 \tag{17}$$

This quadratic expression corresponds to the top curve in Fig. 6b and is an upper bound to γ_{L_1} for any positive value of $\overline{N}_{d_s}$. Large values of d_s/D are typically asso-

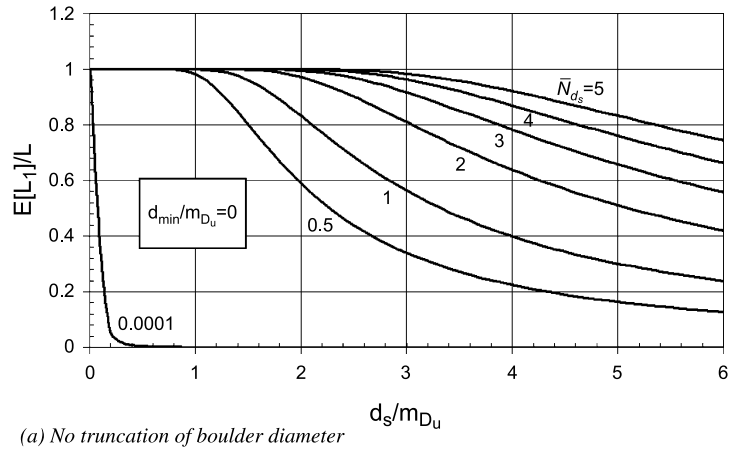

(a) No truncation of boulder diameter

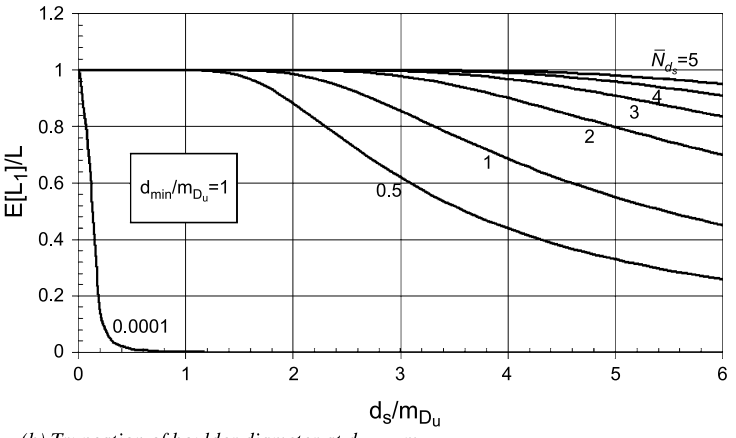

(b) Truncation of boulder diameter at $d_{min} = m_{D_U}$

Fig. 7. Same as Fig. 6a for spherical boulders with exponentially distributed diameter D. The two panels are for (**a**) $d_{min} = 0$ and (**b**) $d_{min} = m_{D_U}$

ciated with large shaft diameters and hence tend to occur with large values of $\overline{N}_{d_s}$. This fact mitigates somewhat the fast increase of γ_{L_1} with the ratio d_s/D.

Figures 7 and 8 show similar results from Eqs. (14) and (15) when the boulder diameter D is random with truncated exponential distribution above d_{min} and moments given in Appendix A. In this case the parameter that is varied on the horizontal axis is the ratio d_s/m_{D_U} where m_{D_U} is the mean diameter in the untruncated case. Since the moments of D in Eq. (15) are the truncated moments of $[D|D \geq d_{\min}]$, the bias factor depends on d_s/m_{D_U}, $d_{\min}$ (or $d_{\min}/m_{D_U}$), and $\overline{N}_{d_s}$. Figures 7 and 8 show results for $d_{min} = 0$ (no truncation) and $d_{min} = m_{D_U}$, and several values of $\overline{N}_{d_s}$.

Comparison of Figs. 7a and 6a shows that randomness in the boulder diameter tends to increase the expected fraction of obstructed shaft length. An additional increase in the obstructed shaft length is observed in the case with truncation from

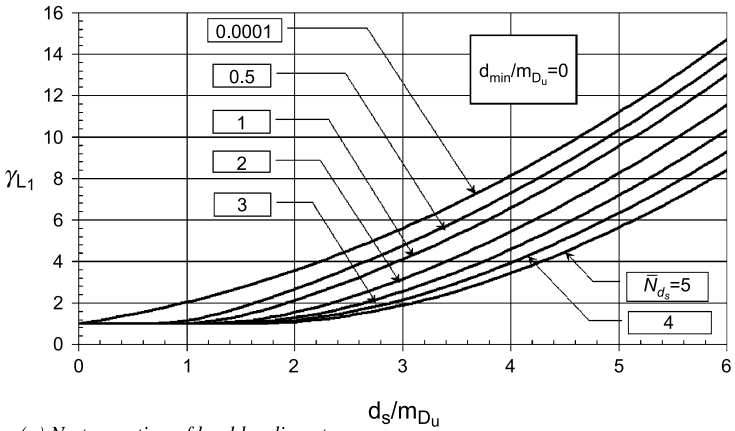

(a) No truncation of boulder diameter

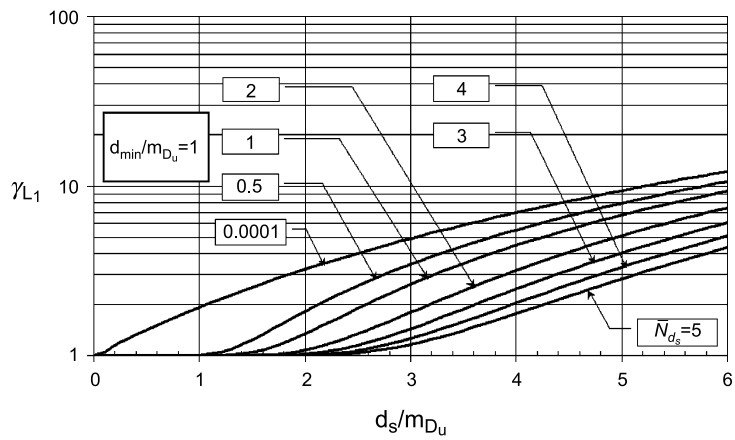

(b) Truncation of boulder diameter at $d_{\min} = m_{D_U}$

Fig. 8. Same as Fig. 6b for spherical boulders with exponentially distributed diameter D. The two panels are for (**a**) $d_{min} = 0$ and (**b**) $d_{min} = m_{D_U}$

below (Fig. 7b), because such operation increases the mean diameter of the obstructing boulders.

The bias factor in Figs. 8a and b follows a trend similar to that in Fig. 6b for the case of constant boulder diameters. The main quantitative difference when D is random is a significant reduction in the size of the bias, meaning that, when D is random, the expected obstructed length is less sensitive to the shaft diameter. The bias is even smaller if the boulder diameter is truncated; see Fig. 8b. In spite of these qualitative trends, the mean length of obstructed shaft may be far greater that the mean length of obstructed small-diameter borings.

(b) Variance of L_1

It follows from Eq. (9) that the variance of L_1 is related to the covariance function of I(z) as

$$\begin{aligned} Var[L_1] &= \int_0^L dz_1 \int_0^L Cov[\,I(z_1),\, I(z_2)]dz_2 \\ &= 2P_0(1-P_0)\int_0^L (L-\Delta)\rho_I(\Delta)d\Delta \end{aligned} \tag{18}$$

where $\rho_I(\Delta)$ is the correlation function of I(z) and use was made of $Cov[I(z), I(z+\Delta)] = Var[I(z)]\ \rho_I(\Delta) = P_0(1-P_0)\ \rho_I(\Delta)$. The correlation function $\rho_I(\Delta)$ is obtained as follows. First we write

$$\begin{aligned} \rho_I(\Delta) &= \frac{Cov[I(z),\ I(z+\Delta)]}{Var[I(z)]} = \frac{E[I(z)I(z+\Delta)] - E^2[I(z)]}{Var[I(z)]} \\ &= \frac{P_{11}(\Delta) - (1-P_0)^2}{P_0(1-P_0)} \end{aligned} \tag{19}$$

Then we express the probability $P_{11}(\Delta)$ in terms of P_0 and $P_{00}(\Delta)$ using

$$\begin{aligned} P_{01}(\Delta) &= P_{10}(\Delta) = P_0 - P_{00}(\Delta) \\ P_{11}(\Delta) &= 1 - P_{00}(\Delta) - 2P_{01}(\Delta)\ = 1 - 2P_0 + P_{00}(\Delta) \end{aligned} \tag{20}$$

Substitution into Eq. (19) gives

$$\rho_I(\Delta) = \frac{1 - 2P_0 + P_{00}(\Delta) - (1-P_0)^2}{P_0(1-P_0)}\ = \frac{P_{00}(\Delta) - P_0^2}{P_0(1-P_0)} \tag{21}$$

The probability P_0 is given by Eq. (13) and the probability $P_{00}(\Delta) = P\{[I(z)=0] \cap [I(z+\Delta)=0]\}$ is obtained by noting that the event $[I(z)=0] \cap [I(z+\Delta)=0]$ occurs if and only if there are no boulder centers of any diameter $D > d_{\min}$ inside regions $\Omega_\Delta(D)$ whose volume $V_\Delta(D)$ is given in Eq. (10). Hence

$$P_{00}(\Delta) = exp\{-\lambda E[V_\Delta(D)]\} \tag{22}$$

While V(D) in Eq. (13) is a polynomial function of D, $V_\Delta(D)$ in Eq. (22) is not; see Eq. (10). Hence the exponent in Eq. (22) cannot be expressed in terms of the first few moments of D and must be evaluated numerically.

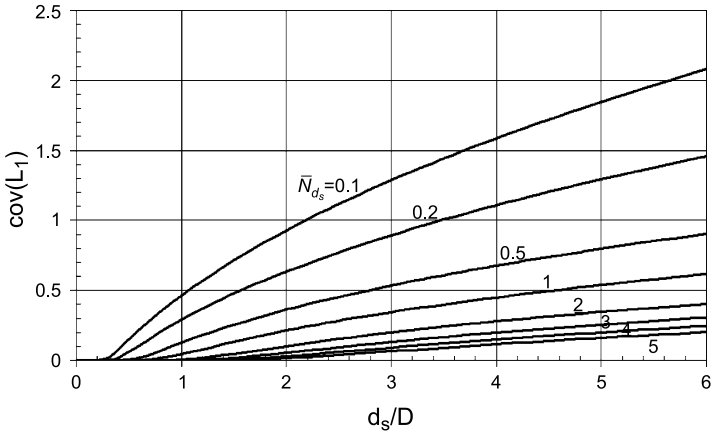

Fig. 9. Coefficient of variation of the length of obstructed drilling L_1, as a function of the dimensionless shaft diameter d_s/D and the mean number $\overline{N}_{d_s}$. The shaft length L is assumed equal to $10\,d_s$

In summary, the variance of the obstructed shaft length L_1 is found by first calculating P_0 and $P_{00}(\Delta)$ in Eqs. (13) and (22). Then the correlation function $\rho_I(\Delta)$ is found from Eq. (21) and the variance of L_1 is obtained from Eq. (18).

Figure 9 shows the coefficient of variation of L_1, $V_{L_1} = \sigma_{L_1}/m_{L_1}$, for the case when the diameter D is the same for all the boulders. This coefficient of variation depends on the ratio d_s/D and the mean number $\overline{N}_{d_s}$ as well as the length L of the shaft, which in Fig. 9 is fixed to $L = 10d_s$.

For small d_s/D ratios and large values of $\overline{N}_{d_s}$, the coefficient of variation is essentially zero. The reason is that under these conditions nearly all the shaft length is expected to be obstructed; see Fig. 6a. Hence the variance of L_1 is very small. For typical values of the parameters, the coefficient of variation remains below 0.5. For example, for $d_s/D = 3$ and $\overline{N}_{d_s} = 2$, the coefficient of variation is about 0.2.

It should be noted that the previous analysis rests on simplifying assumptions and approximations. Equations (18) and (19) neglect the fact that in certain applications one is able to observe and map the outcropping boulders. While one could make corrections to account for this piece of information, the resulting indicator process I(z) would become nonstationary, significantly complicating the analysis. Since the numerical effect of conditioning on knowledge of the boulders above ground level is likely to be small, in the previous analysis we have neglected any such knowledge.

A second potential limitation of the previous analysis is that boulder centers are assumed to have Poisson distribution in space; hence boulder overlap is allowed. Such physical impossibility has small effects on the results if the volume fraction occupied by the boulders, $\lambda \frac{\pi}{6} E[D^3]$, is small relative to 1. If this condition is not met, one should replace the Poisson model with one that prevents boulder overlaps. Several such models exist (see for example Matern, 1986; Diggle, 1983; Cressie, 1991, Sec. 9; and Stoyan et al., 1995, Secs. 5.4 and 6.4) but since their analytical treatment is complicated, one may have to resort to numerical simulation.

3.2 Boulders with Cylindrical and Other Shapes

The solution for cylindrical boulders with height and base diameter both equal to D and axis parallel to the shaft (see Fig. 1b) is especially simple. The mean value and variance of L_1 are still given by Eqs. (14) and (18) and the correlation function $\rho_I(\Delta)$ in Eq. (18) is still given by Eq. (21). The only difference with the spherical case is the value of the volumes V(D) and $V_\Delta(D)$ and hence the probabilities P_0 and $P_{00}(\Delta)$. For cylindrical boulders, these quantities are derived in Appendix C; see Eqs. (C1) and (C2).

It is possible to generalize the previous analysis of spherical and cylindrical boulders to ellipsoids of revolution (prolate or oblate spheroids) and cylinders still with their axis parallel to the shaft but with a vertical height D_z that differs from the horizontal diameter $D_x = D_y = D$. If the ratio $\delta = D_z/D$ is fixed with the same value for all the boulders (meaning that the shape of the boulders is fixed and only their size varies), then the previous results for $\delta = 1$ are readily extended to any given δ. In fact L_1 scales with δ as

$$L_1(\lambda, L, \delta) \stackrel{d}{=} \delta L_1\left(\delta\lambda, \frac{L}{\delta}, 1\right) \tag{23}$$

where $\stackrel{d}{=}$ means that the random variables on the right and left hand sides have the same probability distribution. In particular, the mean value and variance of $L_1(\lambda, L, \delta)$ are given by

$$\begin{aligned} E[L_1(\lambda, L, \delta)] &= \delta E\left[L_1\left(\delta\lambda, \frac{L}{\delta}, 1\right)\right] \\ Var[L_1(\lambda, L, \delta)] &= \delta^2 Var\left[L_1\left(\delta\lambda, \frac{L}{\delta}, 1\right)\right] \end{aligned} \tag{24}$$

where the mean value and variance on the right hand side are obtained as described earlier for $\delta = 1$, using a modified mean density $\lambda' = \delta\lambda$ and a modified shaft length $L' = L/\delta$.

The case when δ is random with independent values from boulder to boulder can also be analyzed. However this more general case is not considered here.

Calculation of the mean value and variance of the total obstructed length L_1 when boulders have complex and variable geometry is much more difficult. When such situations arise, it is recommended to replace the actual boulders with ''equivalent'' simple objects like those examined above. Such replacements, possibly with adjustment of the formulas through appropriate ''shape factors'', is often followed in stereological work; see for example Underwood (1970), Sec. 5.4, or Stoyan et al. (1995), Sec. 11.5.

4. Inference of λ and F_D

In a typical field application, the parameters λ and F_D of the boulder field are not known in advance and must be inferred from boring information. If one idealizes each boring as an observation of the boulder field along a geometrical straight line, then important statistics from which to infer λ and F_D are the rate of boulder encounters along the boring, λ_B, and the distribution of the length of the chord (the intercept of

the boring line with the generic boulder). This inference problem has been rather extensively studied and various nonparametric methods have been developed; see for example Underwood (1970), Sec. 5.4, and Stoyan et al. (1995), Sec. 11.4.2. The discussion that follows considers issues that are relevant to the observation of boulders along boreholes, including the effect of a minimum obstructing diameter $d_{\min}$. Notice that throughout this section $d_{\min}$ is the minimum obstructing diameter in borehole drilling, which may differ from $d_{\min}$ in shaft excavation.

For boreholes of very small diameter, the rate λ_B is given by $\lambda_1(d_s = 0)$ in Eq. (1); hence $\lambda_B = (\pi/4)E[D^2]\lambda$ and one can obtain λ from λ_B as (see also Spektor, 1950; Lord and Willis, 1951; Stoyan et al., 1995, p. 362)

$$\lambda = \frac{4}{\pi E[D^2]}\lambda_B \tag{25}$$

Notice that, in order to use Eq. (25), one must first estimate $E[D^2]$. A method to do so will be given later in this section.

Equation (25) holds for boulders of spherical or cylindrical shape. By contrast, the distribution of the chord length C depends on the shape of the boulders. For cylindrical boulders, the probability density function of C is given by

$$f_C(r) = \frac{r^2}{E[D^2]} f_D(r) \tag{26}$$

whereas for spherical boulders

$$f_C(r) = \frac{2r}{E[D^2]}[1 - F_D(r)] \tag{27}$$

Equation (26) is obtained by noting that the rate at which boulders of diameter D in the range $[r, r + dr]$ are encountered is $(\pi/4)r^2\lambda f_D(r)dr$. Since for cylindrical boulders the chord length C equals the diameter, it follows that $f_C(r) \propto r^2 f_D(r)$, from which Eq. (26) follows. For a derivation of Eq. (27), see Spektor (1950), Lord and Willis (1951), or Stoyan et al. (1995), p. 362. In the case when D has exponential distribution, C in Eq. (27) has Gamma(2) distribution.

One can use Eqs. (26) and (27) to obtain the mean chord length, $E[C]$. In the cylindrical case one finds

$$E[C] = \frac{1}{E[D^2]}\int_0^\infty r^3 f_D(r) = \frac{E[D^3]}{E[D^2]} \tag{28}$$

whereas in the spherical case, integration by parts gives

$$\begin{aligned} E[C] &= \frac{2}{E[D^2]}\int_0^\infty r^2[1 - F_D(r)]dr \\ &= \frac{2}{E[D^2]}\left\{\frac{r^3}{3}[1 - F_D(r)]\Big|_0^\infty + \int_0^\infty \frac{r^3}{3} f_D(r)dr\right\} = \frac{2}{3}\frac{E[D^3]}{E[D^2]} \end{aligned} \tag{29}$$

For a field of boulders of constant diameter D, Eqs. (28) and (29) give $E[C] = C = D$ for cylindrical boulders (in this case C is constant) and $E[C] = 2D/3$ for spherical boulders. Notice that the mean value of C and the moments of D in Eqs. (28) and (29)

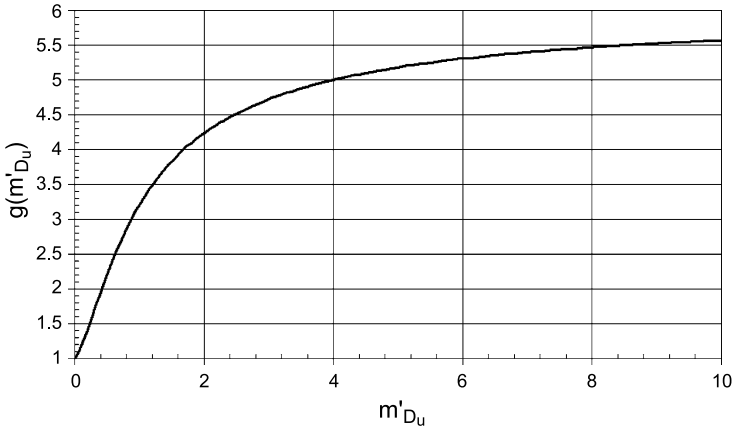

Fig. 10. Plot of the function $g(m'_{D_U})$ in Eq. (30)

refer to the same population of boulders, for example all boulders of diameter $D > 0$ or all boulders with $D \geq d_{\min}$.

Next we evaluate the ratio $E[D^3]/E[D^2]$ in Eqs. (28) and (29) for the case when D has exponential distribution with truncation from below at $d_{\min}$, i.e. we consider $(D|D \geq d_{\min})$. The untruncated mean of D (the mean value of D for $d_{\min} = 0$) is denoted by m_{D_U} and for $d_{\min} > 0$, m'_{D_U} is the dimensionless ratio $m'_{D_U} = m_{D_U}/d_{\min}$. Using Eq. (A3) in Appendix A,

$$\begin{aligned} \frac{E[D^3]}{E[D^2]} &= \frac{d_{\min}^3 + 3d_{\min}^2 m_{D_U} + 6d_{\min} m_{D_U}^2 + 6m_{D_U}^3}{d_{\min}^2 + 2d_{\min} m_{D_U} + 2m_{D_U}^2} \\ &= d_{\min} g(m'_{D_U}) \end{aligned} \tag{30}$$

where $g(x) = \frac{1+3x+6x^2+6x^3}{1+2x+2x^2}$ is plotted in Fig. 10. This figure can be used to estimate m_{D_U} from borehole data, through the following steps:

1. Find the sample average chord length $\overline{C}$
2. Calculate $g = \overline{C}/d_{\min}$ for cylindrical boulders or $g = 3\overline{C}/2d_{\min}$ for spherical boulders
3. Using the plot in Fig. 10, find m'_{D_U} such that $g(m'_{D_U}) = g$
4. Estimate m_{D_U} as $\hat{m}_{D_U} = d_{\min} m'_{D_U}$.

If truncated moments $E[D^r]$ are needed, one should insert $\hat{m}_{D_U}$ into Eq. (A2) or (A3) of Appendix A. In particular, the second moment $E[D^2] = d_{\min}^2 + 2d_{\min} m_{D_U} + 2m_{D_U}^2$ is needed in Eq. (25) to estimate λ from λ_B.

The previous inference procedure is for $d_{\min} > 0$. When $d_{\min} = 0$ (no truncation), $E[D^3]/E[D^2] = 3m_{D_U}$ and Eqs. (28) and (29) give $E[C] = 3m_{D_U}$ for cylindrical boulders and $E[C] = 2m_{D_U}$ for spherical boulders. Hence a simple rule when the boulders are nearly spherical with exponentially distributed diameter and $d_{\min} \ll m_{D_U}$ is to use $\hat{m}_{D_U} = \frac{1}{2}\overline{C}$, where $\overline{C}$ is the average chord length from borehole sampling.

One problem with the above procedure is that the estimator is sensitive to short-chord measurements (Nicholson, 1970). Not only the assumed parametric model for D

(say exponential) may not be accurate for small D, but for small chords the sample may be affected by significant measurement errors. Since interest is mainly in boulders of diameter D larger than a certain size, for example $D > 1$ foot, a better inference procedure may be to ignore all measurements of C below a truncation value $c_{\min}$. If D has exponential distribution with mean value m_{D_U}, then the problem is to estimate the scale parameter m_{D_U} of the $Gamma(2, m_{D_U})$ distribution of C, using a sample from the truncated distribution of $(C|C > c_{\min})$. This problem can for example be solved through maximum likelihood.

5. Conclusions and Extensions

We have examined the problem of boulder encounter during shaft excavation and the bias that results from directly using statistics from borehole samples, without correction for probe diameter. We have focused in particular on two quantities, the rate of boulder encounters λ_1 and the total length of obstructed shaft drilling L_1. We have evaluated analytically how λ_1 and the mean and variance of L_1 depend on the shaft diameter d_s and the boulder size (either the uniform boulder diameter D or the probability distribution of D and the minimum diameter $d_{\min}$ that constitutes an obstruction to drilling). Finally, we have briefly discussed the problem of how to infer the spatial density of boulders λ and their diameter distribution from borehole data.

We have found that both λ_1 and L_1 increase significantly with increasing shaft diameter; hence the uncorrected statistics from borehole samples severely under-predict these two quantities during shaft drilling. For example, if the boulders have a uniform diameter D equal to one half the shaft diameter, the rate λ_1 during shaft excavation is about 9 times the rate during borehole drilling; see Fig. 2. For the same case, the expected length of obstructed excavation may be as high as 12 times the expected length along a borehole; see Fig. 6b. The parameter $\overline{N}_{d_s}$ that appears in Fig. 6b and controls the latter bias factor is the expected number of obstructing boulder centers in a shaft segment of length equal to d_s. Hence $\overline{N}_{d_s}$ depends on the density of boulders in the geologic formation as well as the shaft diameter. It is also interesting that the expected length of obstructed excavation is often a significant fraction of the total shaft length; see Fig. 6a.

The inclusion of variability in the boulder diameter and of a minimum diameter $d_{\min}$ for a boulder to constitute an obstruction reduces the biases mentioned above. For illustration, we have assumed an exponential distribution of boulder diameter and contrasted results under no size limitation ($d_{\min} = 0$) and $d_{\min}$ equal to the mean boulder diameter. The results in Figs. 7 and 8 show that, while significantly reduced, the bias is still large.

In practice, one must also contend with the fact that the length of obstructed shaft drilling L_1 is a random variable (due to the random distribution of boulders in space and their random diameter). We have derived an expression for the variance of L_1 and illustrated this result numerically for the case when the boulders have constant diameter D. For this special case the coefficient of variation of L_1, $Cov[L_1]$, is plotted in Fig. 9. $Cov[L_1]$ is highly sensitive to $\overline{N}_{d_s}$ and to a lesser extent to the dimensionless shaft diameter d_s/D. For typical values of these two parameters and for a shaft length L equal to 10 times the shaft diameter, $Cov[L_1]$ is around 0.2–0.5 and is thus

not negligible. These bias and variance results should be useful to assess when shaft-obstruction statistics are truly inconsistent with results from exploratory borings.

The inference using borehole data of boulder field characteristics like the spatial density λ and the diameter distribution F_D has limited accuracy. The main reason is that boreholes provide information on "chord length", where a chord is the intersection of the borehole (idealized as a line sample) with an individual boulder. The fact that boulders have irregular geometries makes the relation between chord length distribution and diameter distribution complicated and itself uncertain. In addition, chord length measurements are affected by biases and errors, especially for short lengths. We have derived theoretical results for the cases of spherical or cylindrical boulders and suggested a simple inference procedure.

Future studies might investigate how the statistics of the obstructed length L_1 depend on non-Poisson features of the boulder-center distribution and in particular the fact that boulders cannot physically overlap. Other extensions might consider boulders of non-spherical or non-cylindrical shape. It is likely that in all these endeavors analytical tools will be found of limited value, making it necessary to resort to Monte Carlo simulation.

Acknowledgments

This research was supported by the Massachusetts Highway Department. The authors are grateful to Dr. Herbert Einstein for useful comments on an early version of the manuscript and to two anonymous reviewers.

References

Cressie, N. A. C. (1991): Statistics for spatial data. John Wiley & Sons, New York.

Diggle, P. J. (1983): Statistical analysis of spatial point patterns. Academic Press, New York.

Johnson, N. L., Kotz, S. (1970): Distributions in Statistics: Continuous Univariate Distributions, vol. 1. John Wiley & Sons, New York.

Lord, G. W., Willis, T. F. (1951): Calculation of air bubble distribution from results of a rosiwal traverse of aerated concrete. ASTM Bull. 56, 177–187.

Matern, B. (1986): Spatial variation, Lecture Notes in Statistics 36, Springer-Verlag, New York.

Nicholson, W. L. (1970): Estimation of linear properties of particle size distributions. Biometrika 57, 273–297.

Spektor, A. G. (1950): Analysis of distribution of spherical particles in non-transparent structures. Zav. Lab. 16, 173–177.

Stoyan, D., Kendall, W. S., Mecke, J. (1995): Stochastic geometry and its applications. John Wiley & Sons, New York.

Underwood, E. E. (1970): Quantitative stereology. Addison-Wesley, Reading.

Appendix A: Moments of the Truncated Exponential Distribution

Suppose that the untruncated boulder diameter D_U has exponential distribution. Then the truncated diameter $D = (D_U | D_U \geq d_{\min})$ has the same distribution as $D_U + d_{\min}$.

We are interested in how the moments of D depend on $d_{\min}$ and the mean value of D_U, m_{D_U}.

For the untruncated exponential distribution (e.g. Johnson and Kotz, 1970, Chapter 18)

$$E[D_U^r] = r!\, m_{D_U}^r \tag{A1}$$

Then, using the binomial expansion for power functions,

$$\begin{aligned} E[D^r] &= E[(D_U + d_{\min})^r] = \sum_{i=0}^{r} \binom{r}{i} d_{\min}^i E[D_U^{r-i}] \\ &= \sum_{i=0}^{r} r(r-1)\cdots(r-i+1)\, d_{\min}^i m_{D_U}^{r-i} \end{aligned} \tag{A2}$$

In particular, for r = 1, 2 and 3,

$$\begin{aligned} E[D] &= d_{\min} + m_{D_U} \\ E[D^2] &= d_{\min}^2 + 2d_{\min}m_{D_U} + 2m_{D_U}^2 \\ E[D^3] &= d_{\min}^3 + 3d_{\min}^2 m_{D_U} + 6d_{\min}m_{D_U}^2 + 6m_{D_U}^3 \end{aligned} \tag{A3}$$

Appendix B: Derivation of V(D) and V_Δ(D) in Eq. (10)

The volume V of a solid obtained by revolving around the z axis a planar figure delimited by the z axis, the straight lines $z = z_1$ and $z = z_2$, and a non-negative function g(z), $z_1 < z < z_2$, is

$$V = \pi \int_{z_1}^{z_2} [g(z)]^2 dz \tag{B1}$$

In the case of the solid Ω(D), $g(z) = \frac{1}{2}\left(d_s + \sqrt{D^2 - 4z^2}\right)$, $-D/2 < z < D/2$; see Fig. 5a. Hence

$$\begin{aligned} V(D) &= \frac{\pi}{4}\int_{-D/2}^{D/2} \left[d_s^2 + D^2 - 4z^2 + 2d_s\sqrt{D^2 - 4z^2}\right] dz \\ &= \frac{\pi}{4}\left(d_s^2 D + \frac{2}{3}D^3 + 2d_s \int_{-D/2}^{D/2} \sqrt{D^2 - 4z^2}\, dz\right) \end{aligned} \tag{B2}$$

The term $\int_{-D/2}^{D/2} \sqrt{D^2 - 4z^2}\, dz$ equals $\frac{\pi}{4}D^2$, the area of a disc of diameter D. Substitution into Eq. (B2) produces the expression of V(D) in Eq. (10).

Consider now the volume V_Δ(D) of Ω_Δ(D). When $\Delta \geq D$, the two solids of which Ω_Δ(D) is the union do not overlap and $V_\Delta(D) = 2V(D)$. When $\Delta < D$, the solids overlap and V_Δ(D) is twice the volume of the solid of revolution generated by $g(z) = \frac{1}{2}\left(d_s + \sqrt{D^2 - 4z^2}\right)$, $-\Delta/2 < z < D/2$. Hence

$$\begin{aligned} V_\Delta(D) &= \frac{\pi}{2}\int_{-\Delta/2}^{D/2} \left[d_s^2 + D^2 - 4z^2 + 2d_s\sqrt{D^2 - 4z^2}\right] dz \\ &= \frac{\pi}{4}(d_s^2 + D^2)(D + \Delta) - \frac{\pi}{12}(D^3 + \Delta^3) + d_s\pi \int_{-\Delta/2}^{D/2} \sqrt{D^2 - 4z^2}\, dz \end{aligned} \tag{B3}$$

Substitution of $\int_{-\Delta/2}^{D/2} \sqrt{D^2 - 4z^2}\, dz = \frac{1}{4}D^2\left\{\pi - \arccos\left(\frac{\Delta}{D}\right) + \frac{\Delta}{D}\sqrt{1 - \left(\frac{\Delta}{D}\right)^2}\right\}$ gives

$$V_\Delta(D) = \frac{\pi}{4}\left\{(d_s^2 + D^2)(D + \Delta) - \frac{1}{3}(D^3 + \Delta^3)\right\} + \frac{\pi}{4} d_s D^2 \left\{\pi - \arccos\left(\frac{\Delta}{D}\right) + \frac{\Delta}{D}\sqrt{1 - \left(\frac{\Delta}{D}\right)^2}\right\} \tag{B4}$$

which is the expression in Eq. (10).

Appendix C: Mean Value and Variance of L_1 for Cylindrical Boulders

Some simplifications follow from assuming that boulders have cylindrical shape with diameter and height both equal to D and axis parallel to the shaft axis. In this case, the obstructed segments S_{1_i} have length equal to the diameter D of the encountered boulder. This condition simplifies the geometry of the regions $\Omega(D)$ and $\Omega_\Delta(D)$, which are now cylinders with volume

$$V(D) = \frac{\pi}{4}D(D + d_s)^2 = \frac{\pi}{4}(d_s^2 D + 2d_s D^2 + D^3)$$

$$V_\Delta(D) = \begin{cases} 2V(D) = \dfrac{\pi}{2}(d_s^2 D + 2d_s D^2 + D^3), & \text{if } \Delta \geq D \\ \dfrac{\pi}{4}(D + \Delta)(D + d_s)^2 & \\ = \dfrac{\pi}{4}\{d_s^2\Delta + d_s(2\Delta + d_s)D + (\Delta + 2d_s)D^2 + D^3\}, & \text{if } \Delta < D \end{cases} \tag{C1}$$

It follows that the probabilities P_0 and $P_{00}(\Delta)$ are given by

$$P_0 = e^{-\frac{\pi}{4}\lambda\{d_s^2 E_{d_{\min}}[D] + 2d_s E_{d_{\min}}[D^2] + E_{d_{\min}}[D^3]\}}$$

$$P_{00}(\Delta) = \begin{cases} e^{-\frac{\pi}{2}\lambda\{d_s^2 E_{d_{\min}}[D] + 2d_s E_{d_{\min}}[D^2] + E_{d_{\min}}[D^3]\}}, & \text{if } \Delta \geq D \\ e^{-\frac{\pi}{4}\lambda\{d_s^2\Delta + d_s(2\Delta + d_s) E_{d_{\min}}[D] + (\Delta + 2d_s) E_{d_{\min}}[D^2] + E_{d_{\min}}[D^3]\}}, & \text{if } \Delta < D \end{cases} \tag{C2}$$

where $d_{\min}$ is the minimum diameter that can cause obstruction to drilling. Notice that in this case both probabilities in Eq. (C2) depend on the distribution of boulder diameter through only the first three moments of D (limited to $D > d_{\min}$).

Except for these changes, the analysis for cylindrical boulders is identical to that for spherical boulders.

Authors' address: Prof. Daniele Veneziano, Department of Civil and Environmental Engineering, MIT, 77 Massachusetts Avenue, Room 1-348, Cambridge, MA 02139, U.S.A.; e-mail: venezian@mit.edu